

Charge-density-wave order takes over antiferromagnetism in $\text{Bi}_2\text{Sr}_{2-x}\text{La}_x\text{CuO}_6$ superconductors

S. Kawasaki,^{1,*} Z. Li,^{2,*} M. Kitahashi,¹ C. T. Lin,³ P. L. Kuhns,⁴ A. P. Reyes,⁴ and Guo-qing Zheng^{1,2,†}

¹*Department of Physics, Okayama University, Okayama 700-8530, Japan*

²*Institute of Physics, Chinese Academy of Sciences,*

and Beijing National Laboratory for Condensed Matter Physics, Beijing 100190, China

³*Max-Planck-Institut für Festkörperforschung, Heisenbergstrasse 1, D-70569 Stuttgart, Germany*

⁴*National High Magnetic Field Laboratory, Tallahassee, Florida 32310, USA*

(Dated: December 14, 2024)

High temperature superconductivity appears in the cuprates when a spin order is destroyed, while the role of charge is less known. Recent experimental progress suggests that the spin and charge degrees of freedom are highly entangled, which may lead to the enigmatic normal-state pseudogap that spans from the parent antiferromagnetic (AF) insulating phase to the overdoped superconducting regime. For example, short-range charge density wave (CDW) sets in right at the pseudogap temperature T^* in single-layered $\text{Bi}_2\text{Sr}_{2-x}\text{La}_x\text{CuO}_{6+\delta}$, below which spin fluctuations are suppressed. Previously, high magnetic fields have been applied perpendicular to the CuO_2 plane to suppress superconductivity and to diagnose the interplay between spin and charge. Here, we demonstrate, for the first time, that a magnetic field parallel to the plane can be used to tune the electronic state of the cuprates. By ^{63}Cu -nuclear magnetic resonance, we discovered a long-range CDW, setting in above the superconducting dome, under an in-plane field $H_{\parallel} > 10$ T in $\text{Bi}_2\text{Sr}_{2-x}\text{La}_x\text{CuO}_{6+\delta}$. The doping dependence of the onset temperature T_{CDW} traces the T^* curve but down-shifts in temperature, which suggests that the pseudogap is a fluctuating form of the long-range order that we found. The T_{CDW} smoothly takes over the AF order temperature T_N beyond a critical doping level at which superconductivity starts to emerge. These results provide important insights into the relationship between spin order, CDW and the pseudogap, and their connections to high-temperature superconductivity.

High transition-temperature (T_c) superconductivity is obtained by doping carriers to destroy an AF spin ordered Mott insulating phase. Although it is generally believed that the interaction responsible for the spin order is important for the superconductivity [1], the electron pairing mechanism is still elusive. This is because the nature of the normal state is still unclear [2, 3]. For example, in the region with low carrier concentration p ($0 < p < 0.2$), a pseudogap state emerges where partial density of states (DOS) is lost below a characteristic temperature T^* well above T_c [4] or even T_N [5]. Although the nature of the strange metallic state is still under debate, it is likely connected to both spin and charge fluctuations or even orders.

For example, a striped spin/charge order was found around $x \sim 1/8$ in $\text{La}_{2-x}\text{Sr}_x\text{CuO}_4$ two decades ago [6]. More recently, various forms of charge order were reported in many other systems. Scanning tunneling microscopy (STM) in $\text{Bi}_2\text{Sr}_2\text{CaCu}_2\text{O}_{8+\delta}$ found a modulation of local DOS in the vortex cores where superconductivity is destroyed [7], which was interpreted as due to halos of incipient CDW localized within the cores [8, 9]. Resonant inelastic x-ray spectroscopy (RIXS) and other measurements found a short-range CDW with a correlation length $\xi_{a,b} \sim 50$ Å in the normal state of many other systems [10–16]. In $\text{Bi}_2\text{Sr}_{2-x}\text{La}_x\text{CuO}_{6+\delta}$ ($\text{Bi}2201$), most intriguingly, the onset temperature of the short-range CDW was found to coincide [12, 14] with T^* that is far above T_c or T_N [5, 17].

Application of a high magnetic field is useful to elucidate the interplay between various orders in the cuprates. When a high magnetic field is applied perpendicular to the CuO_2 plane, superconductivity can be suppressed substantially. In $\text{YBa}_2\text{Cu}_3\text{O}_{7-y}$ (YBCO), ^{63}Cu nuclear magnetic resonance (NMR) at $H=28.5$ T revealed a long-range charge density modulation perpendicular to the CuO -chain in the sample with $p=0.108$ [18]. RIXS also indicated that a high field induces a correlation along the CuO -chain direction and modifies the coupling between CuO_2 bilayers, thus causes a three-dimensional CDW [19, 20]. These observations are consistent with early discovery of a Fermi-surface reconstruction by quantum oscillations [21] and a recent report of a thermodynamic phase transition [22].

These findings have arisen much interests, but the origin of the CDW and its connection to superconductivity is yet unknown. As the long-range CDW onsets below $T_c(H=0)$ and only emerges when the field is applied perpendicular to the CuO_2 plane, a wide-spread speculation is that it is due to incipient CDW in the vortex cores [7] that becomes overlapped as the field gets stronger [11, 13, 23]. In fact, a field as large as 28.5 T applied in the CuO_2 -plane of YBCO did not bring about any long-range CDW [18]. Also, the role of the CuO chain is unclear; in $\text{Bi}_2\text{Sr}_2\text{CaCu}_2\text{O}_{8+\delta}$ without a CuO chain, no long-range CDW was found [24].

In order to clarify the relationship between the intertwined AF spin order, CDW, pseudogap and supercon-

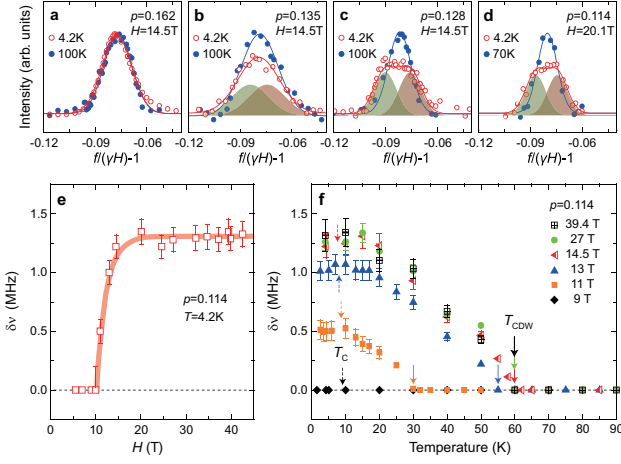


FIG. 1: (a-d) The NMR satellite ($-1/2 \leftrightarrow -3/2$ transition) lines for Bi₂Sr_{2-x}La_xCuO_{6+δ} with $x = 0.4$ ($p = 0.162$), $x = 0.6$ ($p = 0.135$), $x = 0.65$ ($p = 0.128$), and $x = 0.75$ ($p = 0.114$). The curves for $p = 0.135$, 0.128 and 0.114 at $T = 4.2$ K are the sum of two Gaussian functions (shaded area). The horizontal axis is the Knight shift. (e) Field evolution of the line splitting $\delta\nu$ for $p = 0.114$ at $T = 4.2$ K. (f) Temperature evolution of $\delta\nu$ for $p = 0.114$ under various fields. The solid arrows indicate T_{CDW} at different fields, which saturates above 14.5 T. The dotted arrows indicate $T_c(H)$. Error bars include statistical error from the fit.

ductivity, we apply high magnetic fields up to 42.5 T parallel to the CuO₂-plane in Bi₂Sr_{2-x}La_xCuO_{6+δ} that has no CuO chain, without creating vortex cores in the CuO₂ plane. Surprisingly, we discovered a long-range CDW that emerges far *above* the superconducting dome for $H_{\parallel} \geq 10$ T. We find that such CDW order becomes the successor of the AF order beyond $p=0.107$ at which superconductivity starts to emerge. The T_{CDW} smoothly takes over T_N , but disappears well before the pseudogap closes. Our results indicate that CDW can be well disentangled from other orders.

The single crystals of Bi₂Sr_{2-x}La_xCuO_{6+δ} (Bi2201, $p = 0.114$ ($x = 0.75$), 0.128 (0.65), 0.135 (0.60), and 0.162 (0.40)) were grown by the traveling solvent floating zone method [25, 26]. The hole concentration (p) were estimated previously [27]. Small and thin single-crystal platelets, typically sized up to 2 mm-2 mm-0.1 mm, cleaved from an as-grown ingot, were used. The ⁶³Cu-NMR spectra were taken by sweeping the rf frequency at a fixed field below $H = 15$ T but they were taken by sweeping the field at a fixed frequency above $H = 15$ T. High magnetic fields above $H = 15$ T are generated by the Hybrid magnet in the National High Magnetic Field Laboratory, Tallahassee, Florida. For ^{63,65}Cu, the nuclear spin Hamiltonian is expressed as the sum of the Zeeman and nuclear quadrupole interaction terms, $\mathcal{H} = \mathcal{H}_z + \mathcal{H}_Q = -\gamma \hbar \vec{I} \cdot \vec{H}_0(1 + K) + (h\nu_Q/6)[3I_z^2 - I(I+1) + \eta(I_x^2 - I_y^2)]$, where $\gamma = 11.285$ MHz/T

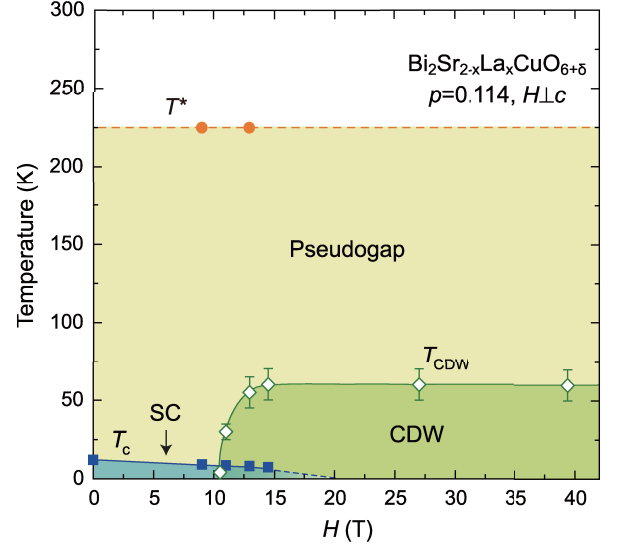


FIG. 2: H - T phase diagram for $p = 0.114$. The T^* is the pseudogap temperature determined from the spin-lattice relaxation rate results. Error bars for T_{CDW} represent the uncertainty in defining the onset of the NMR line splitting.

and $^{65}\gamma = 12.089$ MHz/T, K is the Knight shift, and $I = 3/2$ is the ^{63,65}Cu nuclear spin. The NQR frequency ν_Q and the asymmetry parameter η are defined as $\nu_Q = \frac{3eQV_{zz}}{2I(2I-1)\hbar}$, $\eta = \frac{V_{xx}-V_{yy}}{V_{zz}}$, with Q and $V_{\alpha\beta}$ being the nuclear quadrupole moment and the electric field gradient (EFG) tensor [28]. The principal axis z of the EFG is along the c axis and $\eta = 0$ [29]. Due to \mathcal{H}_Q , one obtains two satellite transition lines between $|m\rangle$ and $|m-1\rangle$ at $\nu_m = (\nu_Q/2)(3\cos^2\theta - 1)(m-1/2)$ in addition to the center line. Here, θ is the angle between \vec{H} and EFG.

Figures 1a-d show the ⁶³Cu-NMR satellite ($-1/2 \leftrightarrow -3/2$ transition) lineshape for four compounds of Bi₂Sr_{2-x}La_xCuO_{6+δ} at two representative temperatures. As seen in Fig. 1a, no change between $T=100$ K and 4.2 K is observed for the optimally-doped compound ($p = 0.162$). However, the spectrum is broadened at $T=4.2$ K for $p = 0.135$ (Fig. 1b), and a clear splitting of the spectrum is observed at $T=4.2$ K for $p=0.128$ and 0.114 , as seen in Figs. 1c and d. The spectra at $T=4.2$ K for $p=0.128$ and 0.114 can be reproduced by a sum of two Gaussian functions, with $\nu = \nu_Q \pm \delta\nu$ where ν_Q is the nuclear quadrupole resonance (NQR) frequency. The obtained $\delta\nu$ is 1.0 MHz and 1.3 MHz for $p=0.128$ and 0.114 , respectively. The same fitting can be applied to the spectrum at $T=4.2$ K for $p=0.135$ with $\delta\nu=0.8$ MHz. This situation is similar to that observed at the in-plane Cu^{2F}-site located below the oxygen-filled CuO chain in YBCO, while the $\delta\nu$ is much smaller (0.3 MHz) there [18]. The NMR line splitting indicates a long-range order, as it measures an assemble of nuclear spins over the sample. It is noted that the possibility of a field-induced

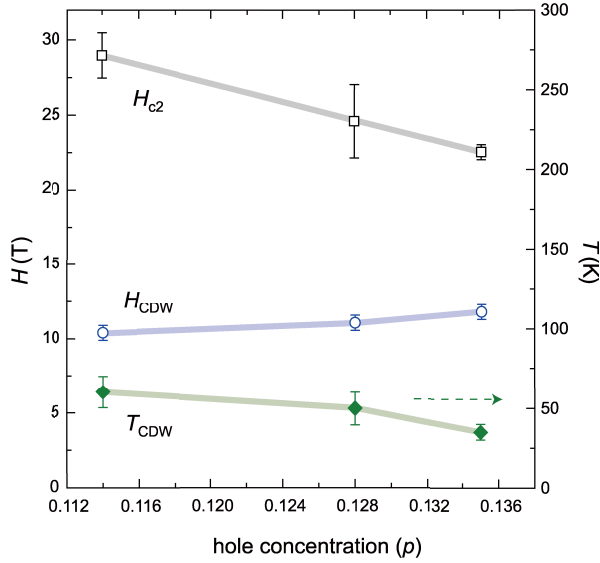


FIG. 3: Doped hole concentration dependence of the upper critical field H_{c2} , H_{CDW} (left axis) and T_{CDW} (right axis). Error bars include statistical error from the fit to obtain H_{c2} and represent the uncertainty in defining the onset of the NMR line splitting for H_{CDW} and T_{CDW} .

spin-density-wave order was ruled out previously [30].

The result can be understood by an incommensurate unidirectional [12] long-range CDW as follows. For an unidirectional CDW state, the wave modulation causes a spatial distribution in the electric field gradient (EFG) and thus the NQR frequency so that $\nu = \nu_Q + \delta\nu \cos(\phi(y))$ [31, 32], where y is the modulation direction. The NMR spectral intensity ($I(\nu)$) depends on the spatial variation of $\phi(y)$ as $I(\nu) = 1/(2\pi d\nu/d\phi)$. For an incommensurate order, $\phi(y)$ is proportional to y , so that the NMR spectrum shows an edge singularity at $\nu = \nu_Q \pm \delta\nu$, as $I(\nu) = 1/(2\pi\delta\nu\sqrt{1-X^2})$ where $X = (\nu - \nu_Q)/\delta\nu$ [31, 32]. By convoluting a broadening function, a two-peak structure can be reproduced. The splitting is also compatible with the EFG modulation expected by the density-wave with the ordering vectors $\vec{q}_{DW} = (0.25, 0)$ and $(0, 0.25)$ inferred from the STM measurement [33].

In such case, the quantity $2\delta\nu$ corresponds to the CDW order parameter [32]. We emphasize that the value of $\delta\nu(T = 0)$ is 3~5 times larger than that observed in YBCO [18], indicating that a much larger CDW amplitude is realized in Bi2201. This difference may arise from the different crystal structure between the two systems. YBCO is a bi-layer system while Bi2201 is single-layered. When CDW has a different phase between two CuO_2 planes, the ordering effect would be weakened or even canceled out.

To obtain the CDW onset temperature (T_{CDW}) and the threshold field (H_{CDW}), we study the temperature dependence of the NMR spectra at various magnetic fields.

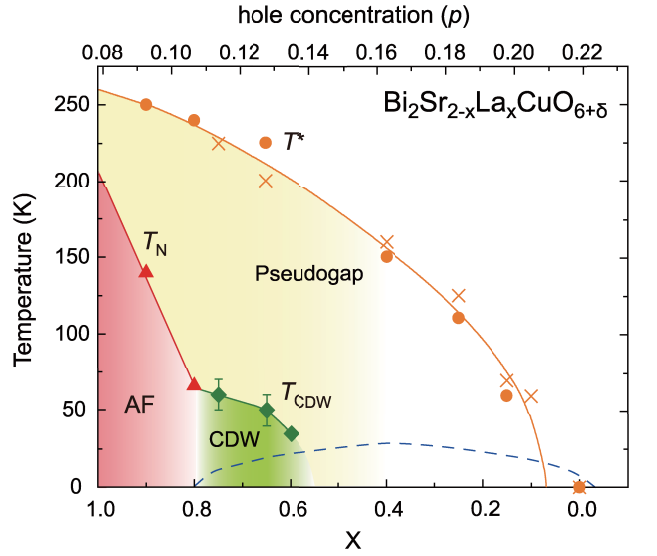


FIG. 4: T - x phase diagram of Bi2201. The T_{CDW} data are the saturated values at $H=14.5$ T. The data for the pseudogap and AF spin ordered temperatures (T^* and T_N) are from previous works [5, 17], which are field-independent. The yellow shaded region below T^* represents short-range CDW reported by the x-ray measurements at zero magnetic field [12, 14]. The dotted curve depicts the zero-field T_c . Error bars represent the uncertainty in defining the onset of the NMR line splitting.

Figure 1e shows the field evolution of $\delta\nu$ for $p = 0.114$. The $\delta\nu$ grows steeply at $H_{CDW} = 10.4$ T and saturates above $H \sim 14.5$ T. Slightly higher $H_{CDW} = 11.0$ and 11.8 T were obtained for $p = 0.128$ and 0.135 , respectively.

Figure 1f shows the temperature dependence of $\delta\nu$ for $p = 0.114$ under various fields. The $\delta\nu$ grows rapidly below $T_{CDW} \sim 30, 55$, and 60 K at $H = 11, 13$, and above 14.5 T, respectively. Figure 2 shows the H - T phase diagram for this compound. Remarkably, the long-range CDW state in Bi2201 emerges at a temperature far above T_c , in contrast to that in YBCO where CDW appears below $T_c(H = 0)$ [18, 23].

The H_{CDW} is slightly lower than that in YBCO, suggesting that CDW has a similar energy scale across different class of cuprates. However, the relationship between H_{CDW} and H_{c2} is completely different from that seen in YBCO where H_{CDW} scaled with H_{c2} . Namely, H_{CDW} was the lowest at the doping concentration where H_{c2} was the smallest there [23], which led to the suggestion that CDW can only be seen when the superconducting state is suppressed. In the present case, however, H_{CDW} and T_{CDW} are more related with doping concentration itself as can be seen in Fig. 3, rather than with H_{c2} . Namely, the long-range CDW order is induced more easily closer to the AF phase boundary.

Finally, we show in Fig. 4 the doping evolution of T_N , T^* , T_{CDW} and T_c . Upon increasing doping, the AF

state with $T_N = 66$ K at $p = 0.107$ changes to a CDW ordered state with $T_{CDW} \sim 60$ K at $p = 0.114$. Upon further doping to $p = 0.162$ where the pseudogap persists, however, the CDW order disappears.

Figure 4 reveals several important things. First and most remarkably, down-shifting the T^* curve in temperature coincides with the T_{CDW} curve, which suggests that the pseudogap is a fluctuating form of the long-range order found in this work. Second, T_N is succeeded smoothly by T_{CDW} beyond a critical doping level at which superconductivity emerges, pointing to the important role of charge degree of freedom in high-temperature superconductivity. This result further calls for scrutinies of the AF insulating phase. In fact, the entanglement of the spin and charge freedoms [3, 34] was recently found to occur already in the insulating phase [35]. Our results show that CDW order is another outstanding quantum phenomenon that needs to be addressed on the same footing as the AF spin order. Finally, the first demonstration of the ability of using an in-plane field to tune the electronic state should stimulate more works that will eventually help to solve the problem of high- T_c superconductivity.

We thank D.-H. Lee, S. Uchida, L. Taillefer, T. K. Lee, M.-H. Julien and S. Onari for useful discussion. A portion of this work was performed at National High Magnetic Field Laboratory, which is supported by NSF Cooperative Agreement No. DMR-1157490 and the State of Florida. Support by research grants from Japan MEXT (No. 25400374 and 16H04016) and MOST of China (No. 2016YFA0300502 and No. 2015CB921304) is acknowledged.

* These authors contributed equally.

† To whom correspondence should be addressed; E-mail: gqzheng123@gmail.com

- [1] P. A. Lee, N. Nagaosa, and X.-G. Wen, *Rev. Mod. Phys.* **78**, 17 (2006).
- [2] B. Keimer *et al.*, *Nature* **518**, 179 (2015).
- [3] E. Fradkin, S. A. Kivelson, and J. M. Tranquada, *Rev. Mod. Phys.* **87**, 457 (2015).
- [4] T. Timusk and B. Statt, *Rep. Prog. Phys.* **62**, 61 (1999).
- [5] S. Kawasaki *et al.*, *Phys. Rev. Lett.* **105**, 137002 (2010).
- [6] J. M. Tranquada *et al.*, *Nature* **375**, 561 (1995).
- [7] J. E. Hoffman *et al.*, *Science* **295**, 466 (2002).
- [8] T. Zhang, E. Demler, and S. Sachdev, *Phys. Rev. B* **66**, 094501 (2002).
- [9] S. A. Kivelson *et al.*, *Phys. Rev. B* **66**, 144516 (2002).
- [10] G. Ghiringhelli *et al.*, *Science* **337**, 821 (2012).
- [11] J. Chang *et al.*, *Nature Phys.* **8**, 871 (2012).
- [12] R. Comin *et al.*, *Science* **343**, 390 (2014).
- [13] E. H. da Silva Neto *et al.*, *Science* **343**, 393 (2014).
- [14] Y. Y. Peng *et al.*, *Phys. Rev. B* **94**, 184511 (2016).
- [15] M. Hashimoto *et al.*, *Phys. Rev. B* **89**, 220511(R) (2014).
- [16] W. Tabis *et al.*, *Nat. Commun.* **5**, 5875 (2014).
- [17] G.-q. Zheng *et al.*, *Phys. Rev. Lett.* **94**, 047006 (2005).
- [18] T. Wu *et al.*, *Nature* **477**, 191 (2011).
- [19] S. Gerber *et al.*, *Science* **350**, 949 (2015).
- [20] J. Chang *et al.*, *Nat. Commun.* **7**, 11494 (2016).
- [21] N. Doiron-Leyraud *et al.*, *Nature* **447**, 565 (2007).
- [22] D. LeBoeuf *et al.*, *Nature Phys.* **9**, 79 (2013).
- [23] T. Wu *et al.*, *Nat. Commun.* **4**, 2113 (2013).
- [24] J. Crocker *et al.*, *Phys. Rev. B* **84**, 224502 (2011).
- [25] J. B. Peng and C. T. Lin, *J. Supercond. Nov. Magn.* **23**, 591 (2010).
- [26] B. Liang and C. T. Lin, *J. Cryst. Growth* **267**, 510 (2004).
- [27] S. Ono *et al.*, *Phys. Rev. Lett.* **85**, 638 (2000).
- [28] A. Abragam, *The principles of nuclear magnetism* (Oxford University Press, London, 1961).
- [29] G.-q. Zheng *et al.*, *J. Phys. Soc. Jpn.* **64**, 2524 (1995).
- [30] J.-W. Mei *et al.*, *Phys. Rev. B* **85**, 134519 (2012).
- [31] R. Blinc, *Phys. Rep.* **79**, 331, (1981).
- [32] S. Kawasaki *et al.*, *Phys. Rev. B* **91**, 060510(R) (2015).
- [33] K. Fujita *et al.*, *PNAS* **111**, E3026 (2014).
- [34] W.L. Tu and T. K. Lee, *Sci. Rep.* **6**, 18675 (2016).
- [35] P. Cai *et al.*, *Nature Phys.* **12**, 1047(2016).